Pleiotropy drives repeatability in the genetic basis of adaptation

Paul Battlay[1], Sam Yeaman[2], Kathryn A. Hodgins[1]

1. School of Biological Sciences, Monash University, Melbourne, Victoria, Australia

2. Department of Biological Sciences, University of Calgary, Calgary, Alberta, Canada

Abstract

Studies of trait-mapping and local adaptation often identify signatures of genetically parallel evolution, where different species evolve similar phenotypes using the same genes. Such patterns appear incongruent with current estimations of quantitative trait architecture. With hundreds or thousands or genes contributing to a trait, why would selection make repeated use of the same genes? Here, we use individual-based simulations to explore a two-patch model with quantitative, pleiotropic traits to understand the parameters which may lead to repeated use of a particular locus during independent bouts of adaptation. We find that repeatability can be driven by increased phenotypic effect size, a reduction in trait dimensionality and a reduction in mutational correlations at a particular locus relative to other loci in the genome, and that these patterns are magnified by increased migration between demes. These results suggest that evolutionary convergence can arise from multiple characteristics of a locus, and provide a framework for the interpretation of quantitative signatures of convergence in empirical studies.

Keywords: pleiotropy, parallel evolution, repeatability, migration, simulations

Introduction

Studies of adaptation commonly observe convergent genetic responses, where multiple species independently respond to a given selection pressure with mutations in orthologous genes. These patterns imply a lack of redundancy in the genes available for a selective response, and at first glance seem inconsistent with another common observation: that variation in quantitative traits is explained by a very large number of alleles of small effect, which suggests a high level of redundancy in the genes contributing to quantitative traits.

In the early 20th century, theoretical work by R. A. Fisher demonstrated that the continuous phenotypic variation observed in populations could be explained by a large number of alleles inherited in a Mendelian manner (Fisher 1918), and that selection would favor small-effect changes at large numbers of loci (Fisher 1930). Genome-wide association studies in humans have provided empirical observations of standing variation congruent to Fisher's models of adaptive trait architecture (reviewed in Visscher *et al.* 2017): Associations with hundreds or thousands of genetic variants explain only a modest proportion of trait heritability, with the remaining heritability attributable to even larger numbers of variants with effect sizes too small to detect with current cohorts (or possibly to rare variants that are excluded from many such analyses). But if variation in thousands of genes underpins a given trait, why would we ever observe orthologous genes contributing to adaptation in multiple species, when there are seemingly a myriad of ways to construct the same traits?

In his revisiting of Fisher's model, Kimura (1968) demonstrated that although smaller effect mutations are more likely to be favourable, beneficial mutations of small effect are less likely to fix, as genetic drift biases the contribution of intermediate-effect loci to adaptation. Later, Orr (1998) showed that effect sizes of fixed adaptive mutations during an adaptive walk should be exponential, illustrating the importance of large-effect mutations early in bouts of adaptation to sudden environmental change. The omnigenic model (which posits that all genetic variants in genes expressed in the relevant cell type contribute to a phenotype; Boyle, Li & Pritchard 2017; Liu, Li & Pritchard 2019) also makes the distinction between 'core' genes of larger effect and 'peripheral' genes of small effect (although the latter explains the bulk of trait heritability). Perhaps the simplest explanation for convergent genetic adaptation is if alleles of large effect are disproportionately likely to contribute to adaptation (e.g., because of their fixation probabilities), but only a subset of loci are able to generate alleles of large effect (Orr 2005). Convergence in gene use would then occur if there is long-term conservation of the genotype-

phenotype map and the potential for particular loci to generate alleles of large effect. Certainly, large-effect QTL have been identified in both experimental evolution studies (e.g. McKenzie & Batterham 1994) and natural populations (e.g. Shapiro *et al.* 2004; Doebly *et al.* 2004), and genomic footprints of selective sweeps (Smith & Haigh 1974; Kaplan, Hudson & Langley 1989) provide evidence for strong selection at individual loci. The effects of local adaptation on genetic architecture may further act to increase the likelihood of repeatability, as the contributions of small-effect alleles are disproportionately limited by the swamping effect of gene flow in populations connected by migration (Yeaman & Whitlock 2011). Consequently, convergence in the genetic basis of local adaptation is expected to frequently involve large-effect mutations, particularly when gene flow is high or drift is strong, yet these processes do not overwhelm selection (Yeaman *et al.* 2018).

While alleles of large effect may be favoured early in adaptation or when there is migration-selection balance, their contribution to adaptation can be limited by pleiotropy.
In both Fisher (1930) and Orr's models (1998), mutations are modelled as vectors in multidimensional phenotypic space; therefore mutations with a large effect in a favorable dimension generally deviate too far from the optima in other dimensions to increase overall fitness. Chevin, Martin & Lenormand (2010) expanded these models to incorporate distinct genes which could vary in their pleiotropic properties: specifically the number of traits that mutations would affect, and the correlation in effects of mutations on different traits (the latter being a property that can arise from organization of genes into networks; Hether & Hohenlohe 2014). They demonstrated that repeatability in the genetics of adaptation is an expected consequence of between-locus variation in pleiotropy; convergence may therefore be observed in genes where negative pleiotropic effects are minimized.

Neither local adaptation nor pleiotropy has been extensively studied in terms of their effects on repeatability, so if we are to interpret empirical observations of repeatability, we need a solid grounding in this theory. Here, we utilize individual-based simulations of quantitative trait evolution to understand how the interplay between inter-locus heterogeneity in pleiotropy and migration-selection balance affects genetic convergence. We build on previous models, which have considered adaptation in a single population following an environmental shift, by introducing a second population adapting to a divergent environment, allowing the observation of interactions between migration, effect size and pleiotropy in bouts of local adaptation. We find that increasing effect size or decreasing pleiotropy (both the overall dimensionality as well

89 as mutational correlation) at a given QTL relative to the other QTL will increase repeatability.
90 Moreover we find that increased migration between demes exacerbates the repeatability
91 observed.

Simulations

To study the factors driving repeatability at particular loci in independent bouts of adaptation, we used SLiM software (Haller & Messer 2019) to simulate adaptation to a complex environment that varied across two patches connected by migration. Adaptation within each patch was driven by selection on two (or more) traits: Z_i with an optimum that varied among the patches, and one or more (e.g. Z_j) with the same optimum in each patch.

Traits could be affected by mutations at five genetically unlinked QTL, four QTL with uniform properties and a single QTL with aberrant properties: At one 'focal' QTL, parameter values could be varied independently of the 'non-focal' QTL. For some parameters, simulations were repeated with a total of 20 QTL and one focal QTL (fig. S3). Each QTL consisted of 500bp, and mutations occurred at a rate of 1×10^{-7}, resulting in an expected 10,000 mutations in each of two demes over the 20,000-generation simulation.

QTL mutations affected two or more phenotypes (e.g. Z_i and Z_j); mutational effects for each QTL were drawn from a multivariate normal distribution where the variance was equal to the QTL effect magnitude and the covariance was equal to the QTL mutational correlation multiplied by the effect magnitude.

The following Gaussian function related individual fitness to phenotype:

$$e^{-\frac{(\theta-\Sigma a)^2}{2V_S}}$$

where θ = the phenotypic optimum, Σa = the sum of mutation effects, and V_s = the variance in the fitness function, reflecting the strength of stabilizing selection (set at 125 for all simulations). Overall individual fitness was calculated as the product of fitness values across all phenotypes, and there was no correlational selection between pairs of phenotypes.

We simulated two demes (d_1 and d_2), each composed of 1000 randomly-mating hermaphroditic individuals. Phenotypic space was unitless and provided a relative scaling of fitness vs mutational effect. Both demes began the simulation with phenotypic optima of 0 for all phenotypes and ran with a burn-in for 20,000 generations. After the burn-in, in d_1 the optima for

all phenotypes remained at 0, while in d_2, the optimum for Z_i was shifted to -10, while other phenotypic optima remained at 0, and we tracked adaptive evolution over the following 20,000 generations. We varied the migration rate between d_1 and d_2 (from 0 to 0.05) and the mutation effect magnitudes (from 0.1 to 5), mutational correlations (from 0 to 0.99), and the number of phenotypes affected at the QTL.

To interpret the results of each parameter combination, we calculated the genetic value (*GV*) of each mutation to a phenotype using the formula:

$$GV = (p_1 - p_2) \times a$$

where p_1 and p_2 are the frequencies of a mutation in each deme, and a is the size of the mutation's effect on Z_i

We investigated three main ways in which the characteristics of the focal QTL could be differentiated from those of the other loci:

1) A change in effect magnitude by altering the variance component of the variance-covariance matrix used to generate mutations (fig. 1A cf. B). This parameter was used to model a large-effect QTL at the focal QTL.
2) A change in mutational correlation by altering the covariance component of the variance-covariance matrix (fig 1A cf. C). This parameter models dependence between phenotypes and determines the likelihood that a mutation's effect on one phenotype will have a corresponding effect on another.
3) A change in the number of phenotypes affected by a mutation by reducing the dimensionality of the variance-covariance matrix (fig. 1A cf. D). This models a situation where a QTL has no effect on one or more phenotypes..

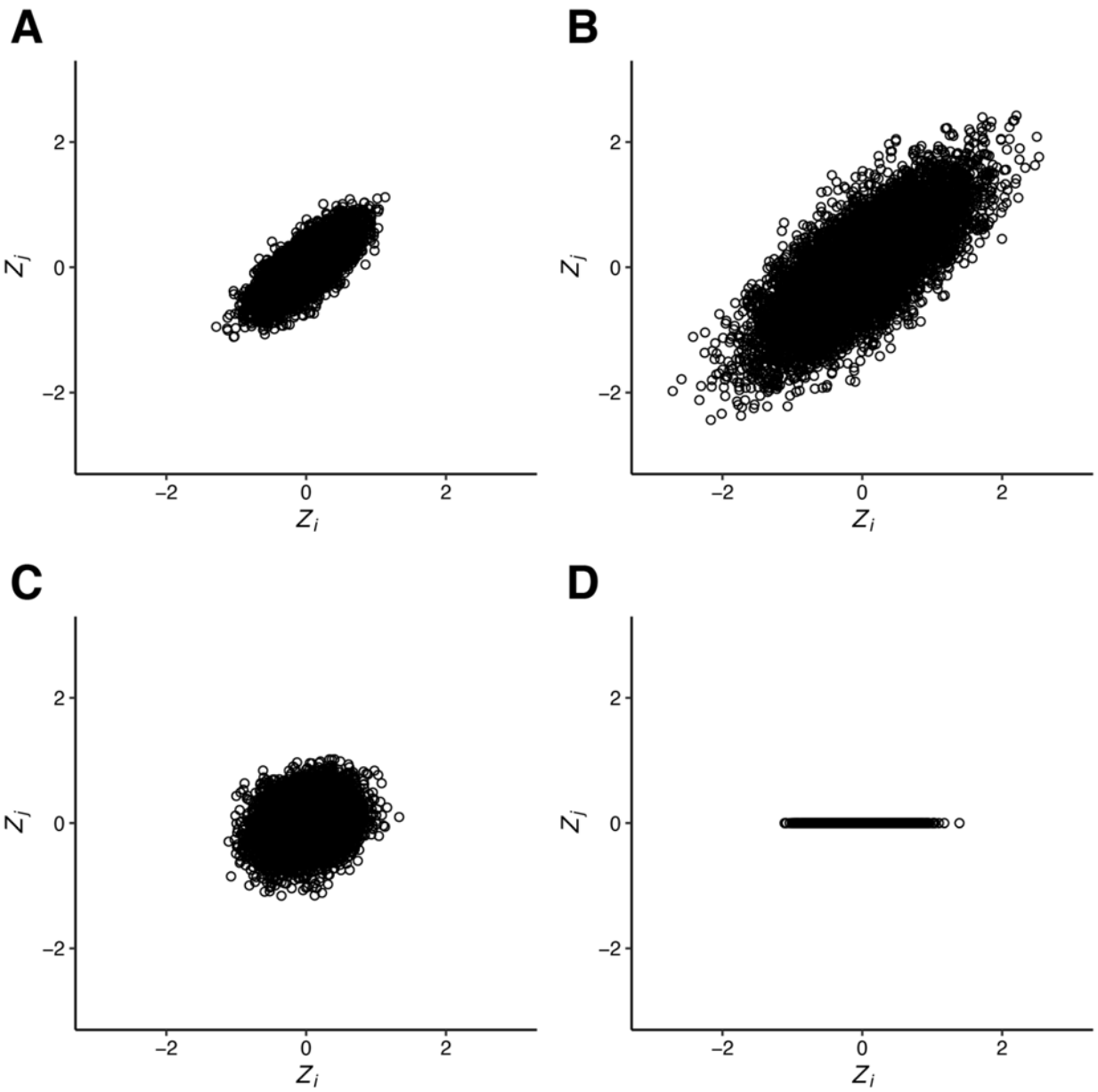

Figure 1. Effect sizes on Z_i (x-axes) and Z_j (y-axes) for 10,000 draws from distributions used to generate mutations. In A, the mean effect magnitude is 0.1 and the mutational correlation between traits is 0.75. In B, the mutational correlation is the same as A (0.75) but the mean effect magnitude is increased to 0.5. In C, the mean effect magnitude is the same as A (0.1), but the mutational correlation is relaxed to 0.25. In D, mutations have no effect on the non-divergent phenotype.

For each parameter combination we quantified the divergence between demes d_1 and d_2 at the divergently selected phenotype by summing $2 \times GV$ across all individuals, and quantified repeatability in the contributions of the QTL to trait divergence (measured by QTL-specific GV) across 100 replicates using the C_{chisq} statistic with 1000 permutations (Yeaman *et al.* 2018). Briefly, χ^2 was calculated across simulation replicates with:

$$\chi^2 = \frac{\Sigma(\underline{\alpha_i} - \underline{\underline{\alpha}})^2}{\underline{\underline{\alpha}}}$$

where $\underline{\alpha_i}$ is the sum across simulation replicates of GV for the i^{th} QTL, and $\underline{\underline{\alpha}}$ is the mean $\underline{\alpha}$ across all QTL.

The C_{chisq} statistic was then calculated by using χ^2 and χ^2_{sim}, the results of 1000 permutations of the data within each replicate:

$$C_{chisq} = \frac{\chi^2 - mean(\chi^2_{sim})}{sd(\chi^2_{sim})}$$

By this equation, when $C_{chisq} = 0$ we observe no excess repeatability, and complete repeatability is observed for five QTL when $C_{chisq} = 2$.

Additionally, we calculated $GV_{focal} / GV_{non\text{-}focal}$, the ratio of GV at the focal QTL to the mean GV across non-focal QTL.

Results

To model the case where the focal QTL is more important to the divergent phenotype than the non-focal QTL, we examined the effect of varying the effect magnitude at the focal QTL while holding effect magnitude constant at non-focal QTLs. The genes involved in adaptation are random (C_{chisq} = 0) when all loci have the same mutation effect size and correlation (fig. 2 where focal QTL effect magnitude = 0.1). Increased repeatability was observed with any increase in focal QTL effect magnitude (fig. 2) across all mutational correlation and migration rate values. Additionally, increasing migration rates resulted in increasing repeatability (fig. 2; fig. S1), and this pattern was exacerbated by increasing mutational correlations.

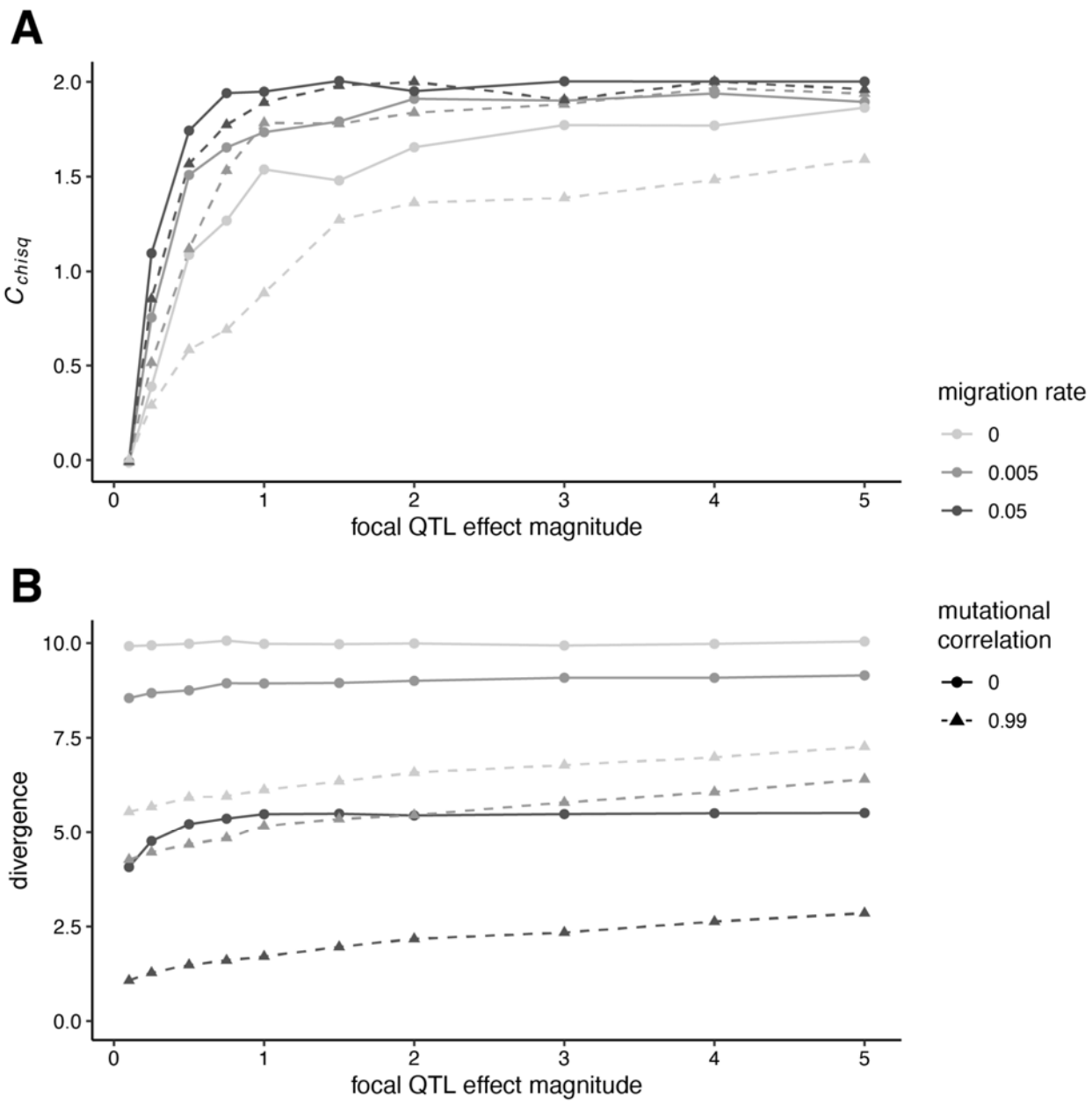

Figure 2. Repeatability (C_{chisq}) in Z_i (A) and Z_i phenotypic divergence between d_i and d_j (B) against focal QTL effect magnitude where the effect magnitude for non-focal QTL is 0.1, and where mutational correlations between phenotypes at all QTL are 0 (circle points; solid lines) or 0.99 (triangle points; dashed lines). These simulations use two phenotypes (one divergent and one non-divergent), and were run for 20,000 generations.

Reducing the correlation in phenotypic effects at a QTL may also allow it to more readily acquire adaptive mutations when the direction of change toward the optimum is not aligned with the correlation in phenotypic effects. We modeled this by independently varying mutational correlations at the focal and non-focal QTL (fig. 3; fig. S2), and observed repeatability for mismatches between mutational correlation values (fig. 3). When the mutational correlation at the focal QTL was reduced relative to the non-focal QTL, repeatability involving the focal QTL increased, and when the mutational correlation at the focal QTL was increased relative to the non-focal QTL, repeatability involving the focal QTL decreased (this latter observation was not robust to an increase in the number of QTL [fig. S3]). High levels of repeatability were only seen when the focal QTL had a relaxed mutational correlation against a background of high mutational correlation at non-focal QTL (i.e. 0.75 and particularly 0.9). This reflects the fact that mutational correlations need to be high to significantly limit the availability of fortuitous combinations of effects on the phenotypes at the other QTL.

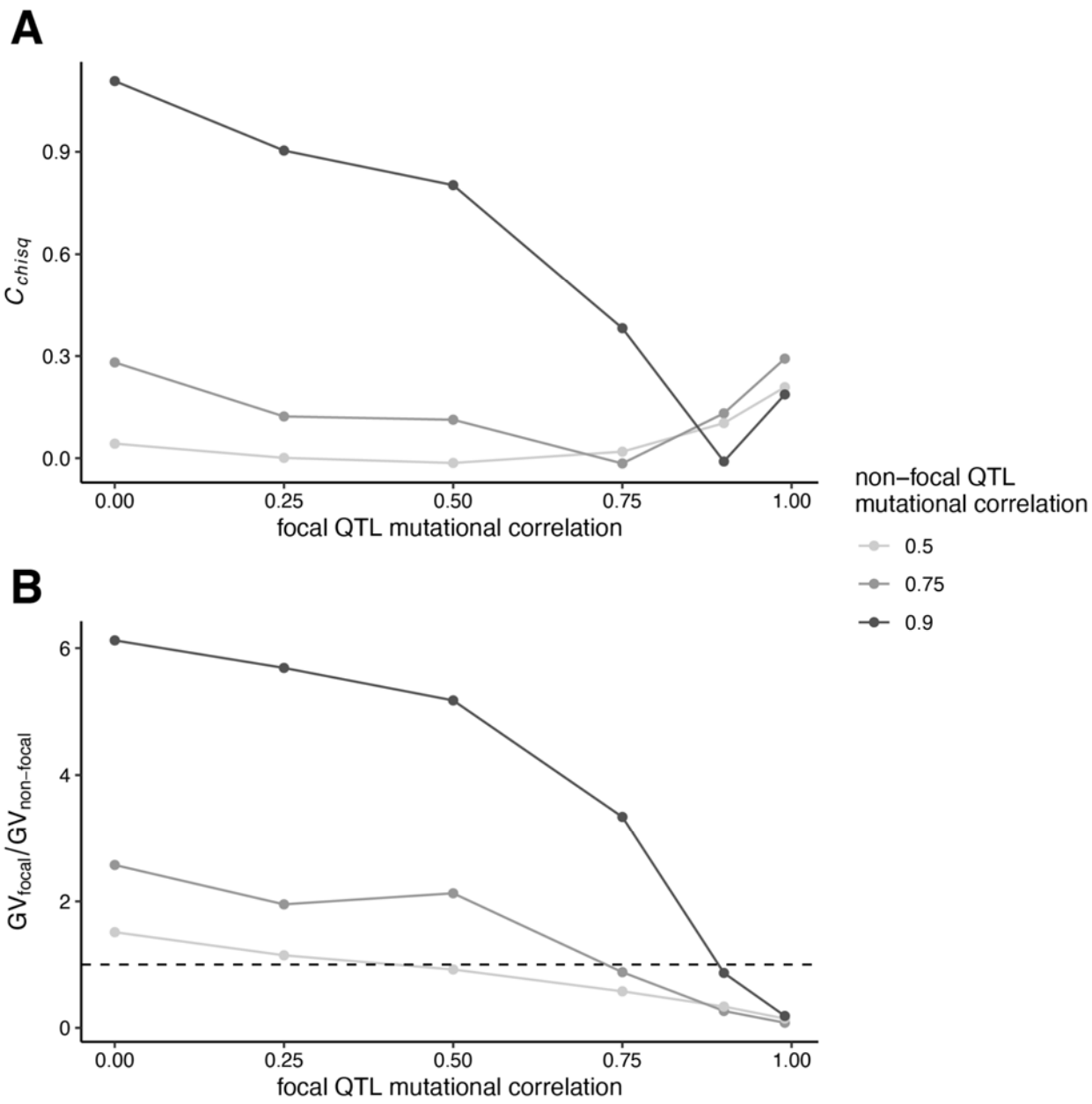

Figure 3. Repeatability (C_{chisq}) in Z_i against focal QTL mutational correlation for varying values of non-focal QTL mutation correlation (A), and corresponding ratios of the *GV* at focal QTL to mean *GV* at non-focal QTL (B). The dotted line indicates $GV_{focal} / GV_{non\text{-}focal} = 1$, the point at which this value shifts from representing overuse of the focal QTL to underuse of the focal QTL. These simulations use a migration rate of 0.005, a mutation effect magnitude of 0.5 and two phenotypes (one divergent and one non-divergent), and were run for 20,000 generations.

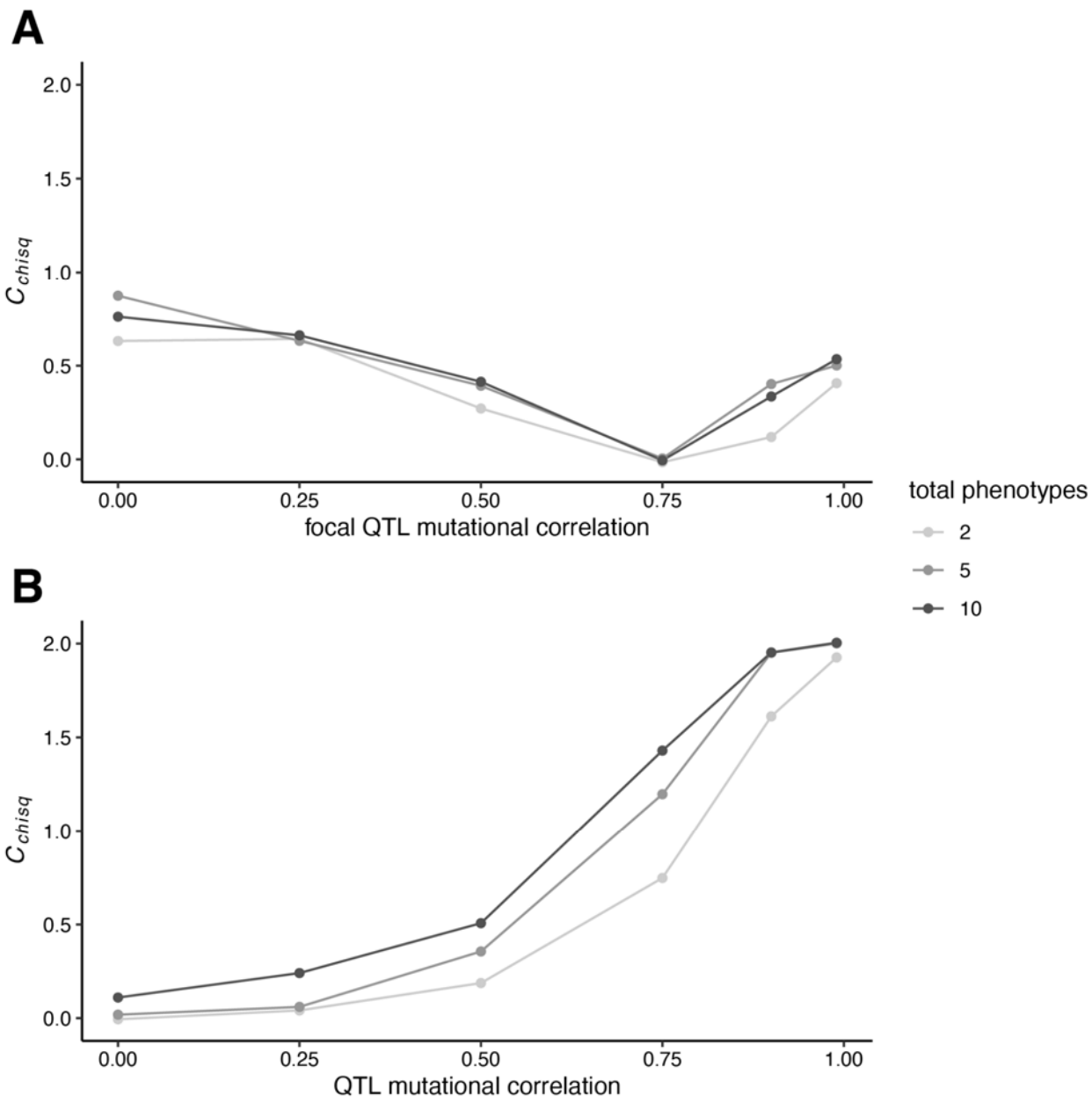

Figure 4. Repeatability (C_{chisq}) against focal QTL mutational correlation where the non-focal QTL mutation correlation = 0.75 (A) and repeatability against QTL mutational correlation where the focal QTL affects the divergent phenotype (Z_i) and one fewer non-divergent phenotypes than the non-focal QTL (B). Shades indicate the total number of phenotypes in the simulation (two with one non-divergent phenotype, five with four non-divergent phenotypes and ten with nine non-divergent phenotypes). These simulations use a migration rate of 0.005 and a mutation effect magnitude of 0.1, and were run for 20,000 generations.

To assess how robust these observations were to an increase in the dimensionality of the model, we increased the number of non-divergent phenotypes from one to nine for the case where the non-focal QTL mutational correlation = 0.75, but saw only a very modest increase in repeatability (fig. 4A). Finally, we investigated the case where mutations at the focal QTL affect fewer phenotypes than the non-focal QTL. In the two-phenotype model, this meant focal QTL mutations would only affect the divergent phenotype; in the five and ten-phenotype models, focal QTL mutations affected the divergent phenotype and one fewer non-divergent phenotypes than non-focal QTL. With high mutational correlation between phenotypic effects, high levels of repeatability at the focal QTL is observed, however when mutational correlations are weak or absent, very little repeatability is observed (fig. 4B).

Discussion

Empirical observations of convergent genetic evolution are common (reviewed in Conte *et al.* 2012), but in many ways at odds with some models of complex trait architecture. In this study we used simulations to understand the factors that could be varied at a QTL to produce convergent evolutionary patterns. Firstly, we demonstrated that an increase in effect magnitude of a QTL will produce patterns of repeatability, which is consistent with previous theoretical (Chevin, Martin & Lenormand 2010) and empirical observations (e.g. Rosenblum, Hoekstra, & Nachman 2004; Schlenke & Begun 2004). Both mutational correlations and migration can force adaptation away from phenotypic optima along 'genetic lines of least resistance' (Schluter 1996; Guillaume 2011). Correspondingly, we see a reduction in divergence between demes as mutational correlations or migration is increased (fig. 2B). However, while increasing mutational correlations reduce repeatability, migration amplifies it (fig. 2A).

We also investigated how varying pleiotropy at the focal locus affected signatures of repeatability. Pleiotropy was varied in two ways: a relaxation in mutational correlations with a non-divergent phenotype, or a reduction in the number of phenotypes that a QTL mutation affects. Congruent with the findings of Chevin, Martin & Lenormand (2010), we found that variation in different forms of pleiotropy will increase the likelihood that repeatability will emerge. Specifically, we find that a reduction in pleiotropic dimensionality at a focal QTL produces greater levels of repeatability than a relaxation in mutational correlations, a pattern that is robust to increases in trait dimensionality in our models (fig. 4A c.f. B).

Whereas Chevin, Martin & Lenormand (2010) used a single phenotype in a single deme under divergent selection, our simulations used two demes linked by varying amounts of migration. This models a common situation in local adaptation: Individuals in one population may experience local environmental shifts; they must therefore adapt to new optima for some phenotypes, while retaining existing optima at others. Previously, Yeaman & Whitlock (2011) demonstrated that migration concentrates the genetic architecture of local adaptation and favors alleles of larger effect. Correspondingly, we find that migration increases the observed repeatability arising from effect-magnitude variation (fig. 2, fig. S1), as high migration rates favour adaptation by larger effect alleles, which can most readily occur at the focal locus when pleiotropy is present. But this effect breaks down at high migration, where swamping tends to prevent persistent divergence. We also find that migration increases repeatability arising from pleiotropic variation (fig. S2). This is because the net effect of selection on a QTL is driving

repeatability. Under migration-selection balance those QTL with larger net beneficial effects (weaker mutational correlations) will be maintained as differentiated when there is migration (unless migration is so high that no mutations meet the threshold).

Guillaume (2011) utilized a similar two-patch design to investigate the effects of pleiotropy and migration on population divergence. He demonstrated that combinations of migration and pleiotropy can drive divergence between demes at phenotypes that share the same optima in both demes, as long as the phenotypes are sufficiently correlated with divergently selected phenotypes. We observe similar patterns in our simulations: Increasing levels of mutational correlations and migration reduce differentiation between demes at the divergent phenotype, and increase differentiation between demes at non-divergent phenotypes. Perhaps surprisingly, this reduced phenotypic differentiation does not necessarily limit genetic repeatability, as high C_{chisq} values are observed in simulations where pleiotropy and migration have substantially limited the divergence between demes (fig. 2).

Our simulations make a number of assumptions that are almost certainly violated in natural populations exhibiting evolutionary convergence. Firstly, we assume complete orthology between QTL in replicates and that orthologous QTL retain corresponding effect magnitude and pleiotropic properties. In nature, divergence between species limits studies of convergence to the orthologous portions of their genomes and the effects of adaptation in non-orthologous regions has not been addressed here. Secondly, we have assumed that both the initial phenotypic optima (to which both demes start our simulations adapted) and the divergent phenotypic optima are identical. Related species adapting to similar environments will not share identical phenotypic optima, which is important for the interpretation of our results, as Thompson, Osmond & Schluter (2019) observed that repeatability declines rapidly as the angle between phenotypic optima increases, a pattern that is exacerbated by increased trait dimensionality. Furthermore variation between QTL in mutation rate, retention of standing variation and patterns of linkage disequilibrium may all affect the likelihood of repeatability, but we have held these parameters constant in our simulations.

The simulations presented here also use a simplified genome architecture: four QTL with uniform properties and a single QTL with aberrant properties, and between two and ten pleiotropic traits. This system pales in comparison to the thousands of genes (exhibiting near-global pleiotropy) which contribute to traits under the omnigenic model (Boyle, Li & Pritchard

2017; Liu, Li & Pritchard 2019). Contrastingly, a metaanalysis of gene knockout experiments in *Saccharomyces cerevisiae*, *Caenorhabditis elegans* and *Mus musculus* (Wang, Liao & Zhang 2010) estimated pleiotropy to be far less pervasive: a median gene affects only one to nine percent of traits. Wang, Liao & Zhang (2010) also detected significant signals of modular pleiotropy (where subsets of genes affect subsets of traits), which would serve to simplify the architecture available for evolutionary convergence. Simple genetic architecture enhances repeatability at a genome-wide level, and this study demonstrates that an even more modular architecture at some QTL will act to further magnify repeatability. While the nature of pleiotropic, quantitative traits in higher organisms remains unresolved, we expect our simple model to be applicable to more complex architectures (Yeaman *et al.* 2018), and repeating our simulations on models with 20 QTL yields comparable results (fig. S3).

References

Boyle, E.A., Li, Y.I. and Pritchard, J.K., 2017. An expanded view of complex traits: from polygenic to omnigenic. *Cell*, *169*(7), pp.1177-1186.

Chevin, L.M., Martin, G. and Lenormand, T., 2010. Fisher's model and the genomics of adaptation: restricted pleiotropy, heterogenous mutation, and parallel evolution. *Evolution: International Journal of Organic Evolution*, *64*(11), pp.3213-3231.

Conte, G.L., Arnegard, M.E., Peichel, C.L. and Schluter, D., 2012. The probability of genetic parallelism and convergence in natural populations. *Proceedings of the Royal Society B: Biological Sciences*, *279*(1749), pp.5039-5047.

Doebley, J., 2004. The genetics of maize evolution. *Annu. Rev. Genet.*, *38*, pp.37-59.

Fisher, R.A., 1918. The correlation between relatives on the supposition of mendelian inheritance. *Transactions of the Royal Society of Edinburgh*, *52*, pp 399-433.

Fisher, R.A., 1930. *The Genetical Theory of Natural Selection*. The Clarendon Press.

Haller, B.C. and Messer, P.W., 2019. SLiM 3: forward genetic simulations beyond the Wright–Fisher model. *Molecular biology and evolution*, *36*(3), pp.632-637.

Hether, T.D. and Hohenlohe, P.A., 2014. Genetic regulatory network motifs constrain adaptation through curvature in the landscape of mutational (co) variance. *Evolution*, *68*(4), pp.950-964.

Kaplan, N.L., Hudson, R.R. and Langley, C.H., 1989. The" hitchhiking effect" revisited. *Genetics*, *123*(4), pp.887-899.

Kimura, M., 1968. Evolutionary rate at the molecular level. *Nature*, *217*(5129), pp.624-626.

Liu, X., Li, Y.I. and Pritchard, J.K., 2019. Trans effects on gene expression can drive omnigenic inheritance. *Cell*, *177*(4), pp.1022-1034.

McKenzie, J.A. and Batterham, P., 1994. The genetic, molecular and phenotypic consequences of selection for insecticide resistance. *Trends in Ecology & Evolution*, *9*(5), pp.166-169.

Orr, H.A., 1998. The population genetics of adaptation: the distribution of factors fixed during adaptive evolution. *Evolution*, *52*(4), pp.935-949.

Orr, H.A., 2005. The probability of parallel evolution. *Evolution*, *59*(1), pp.216-220.

Rosenblum, E.B., Hoekstra, H.E. and Nachman, M.W., 2004. Adaptive reptile color variation and the evolution of the MCIR gene. *Evolution*, *58*(8), pp.1794-1808.

Schlenke, T.A. and Begun, D.J., 2004. Strong selective sweep associated with a transposon insertion in Drosophila simulans. *Proceedings of the National Academy of Sciences*, *101*(6), pp.1626-1631.

Schluter, D., 1996. Adaptive radiation along genetic lines of least resistance. *Evolution*, *50*(5), pp.1766-1774.

Shapiro, M.D., Marks, M.E., Peichel, C.L., Blackman, B.K., Nereng, K.S., Jónsson, B., Schluter, D. and Kingsley, D.M., 2004. Genetic and developmental basis of evolutionary pelvic reduction in threespine sticklebacks. *Nature*, *428*(6984), pp.717-723.

Smith, J.M. and Haigh, J., 1974. The hitch-hiking effect of a favourable gene. *Genetics Research*, *23*(1), pp.23-35.

Visscher, P.M., Wray, N.R., Zhang, Q., Sklar, P., McCarthy, M.I., Brown, M.A. and Yang, J., 2017. 10 years of GWAS discovery: biology, function, and translation. *The American Journal of Human Genetics*, *101*(1), pp.5-22.

Wang, Z., Liao, B. Y., & Zhang, J. (2010). Genomic patterns of pleiotropy and the evolution of complexity. *Proceedings of the National Academy of Sciences*, *107*(42), 18034-18039.

Yeaman, S. and Whitlock, M.C., 2011. The genetic architecture of adaptation under migration–selection balance. *Evolution: International Journal of Organic Evolution*, *65*(7), pp.1897-1911.

Yeaman, S., Gerstein, A.C., Hodgins, K.A. and Whitlock, M.C., 2018. Quantifying how constraints limit the diversity of viable routes to adaptation. *PLoS genetics*, *14*(10), p.e1007717.

Supplementary figures

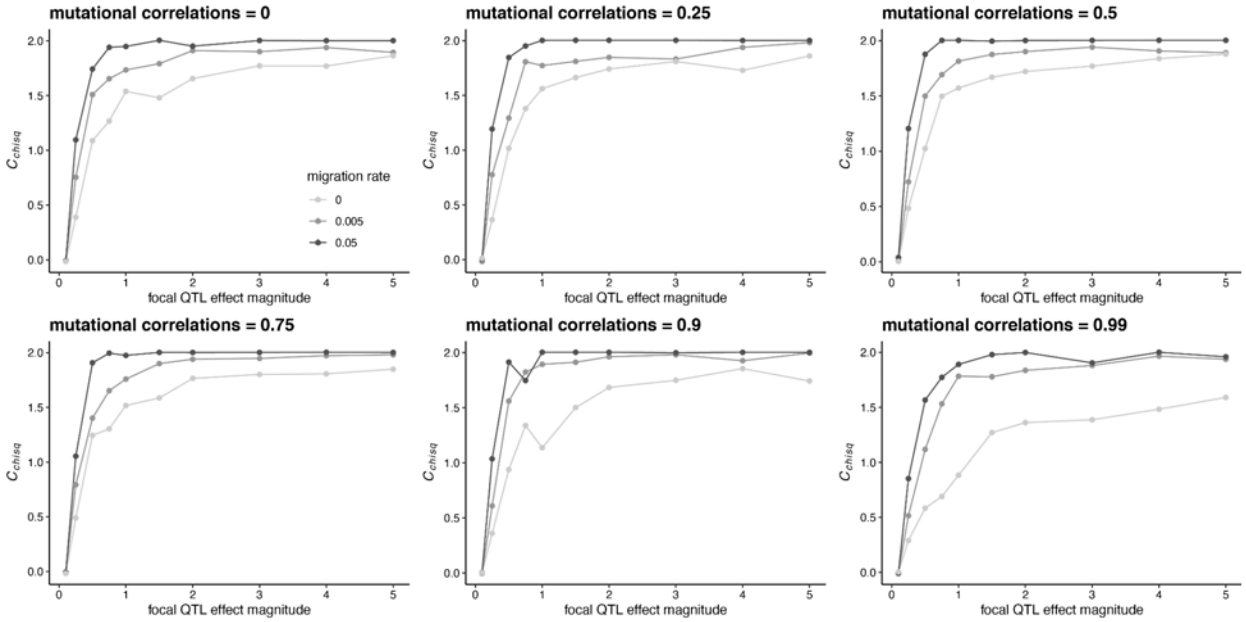

Figure S1. Repeatability (C_{chisq}) in Z_i against focal QTL effect magnitude where the effect magnitude for non-focal QTL is 0.1. These simulations use two phenotypes (one divergent and one non-divergent), and were run for 20,000 generations.

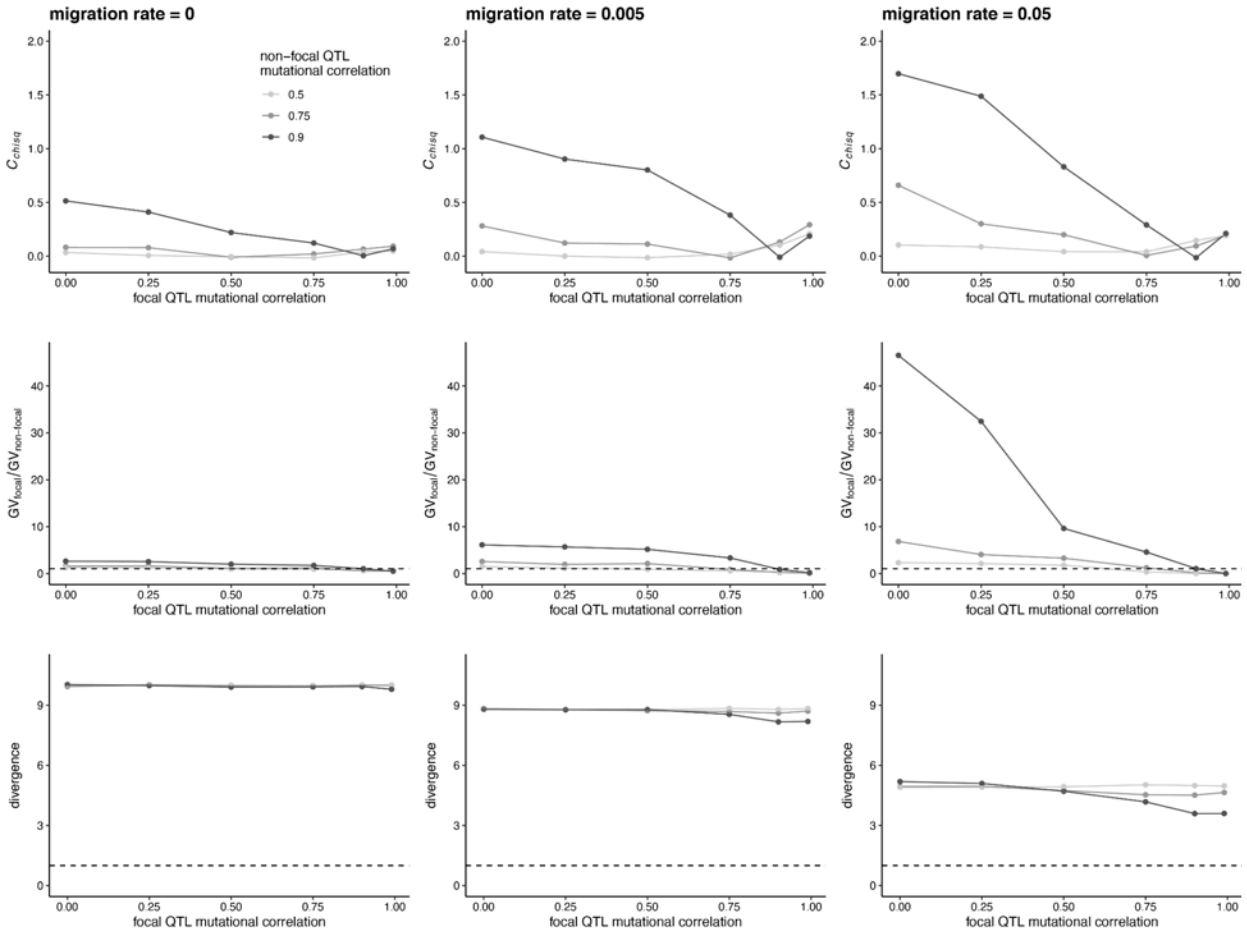

Figure S2. Repeatability (C_{chisq}) in Z_i against focal QTL mutational correlation for varying values of non-focal QTL mutation correlation (top row), corresponding ratios of the *GV* at focal QTL to mean *GV* at non-focal QTL (middle row), and divergence between demes (bottom row). These simulations use a mutation effect magnitude of 0.5 and two phenotypes (one divergent and one non-divergent), and were run for 20,000 generations.

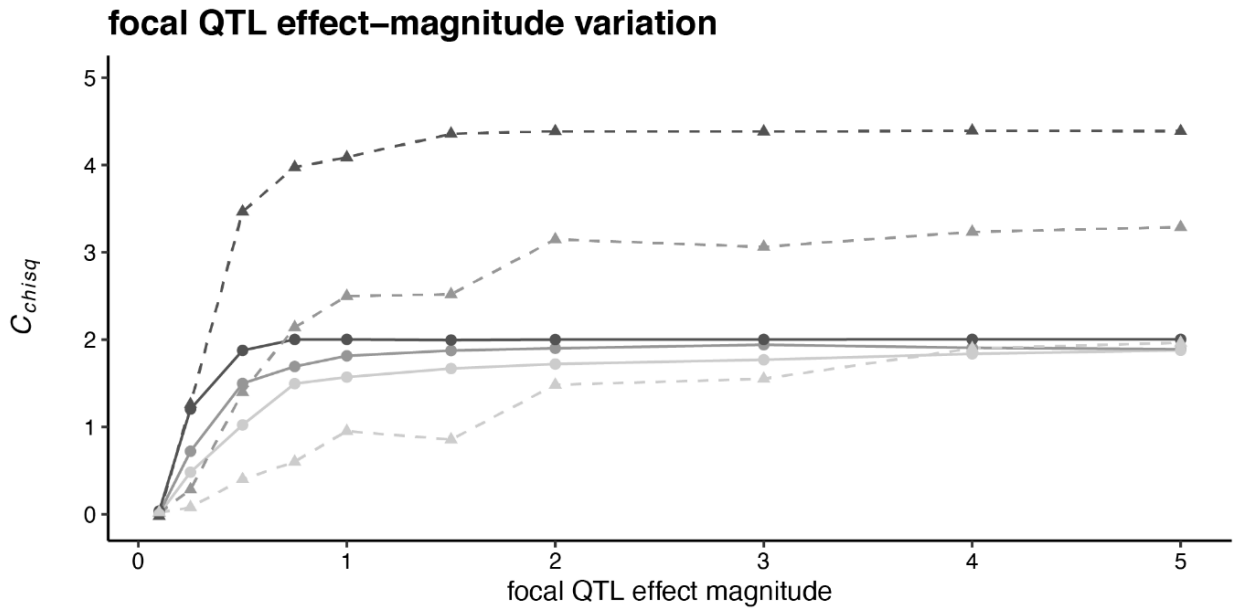

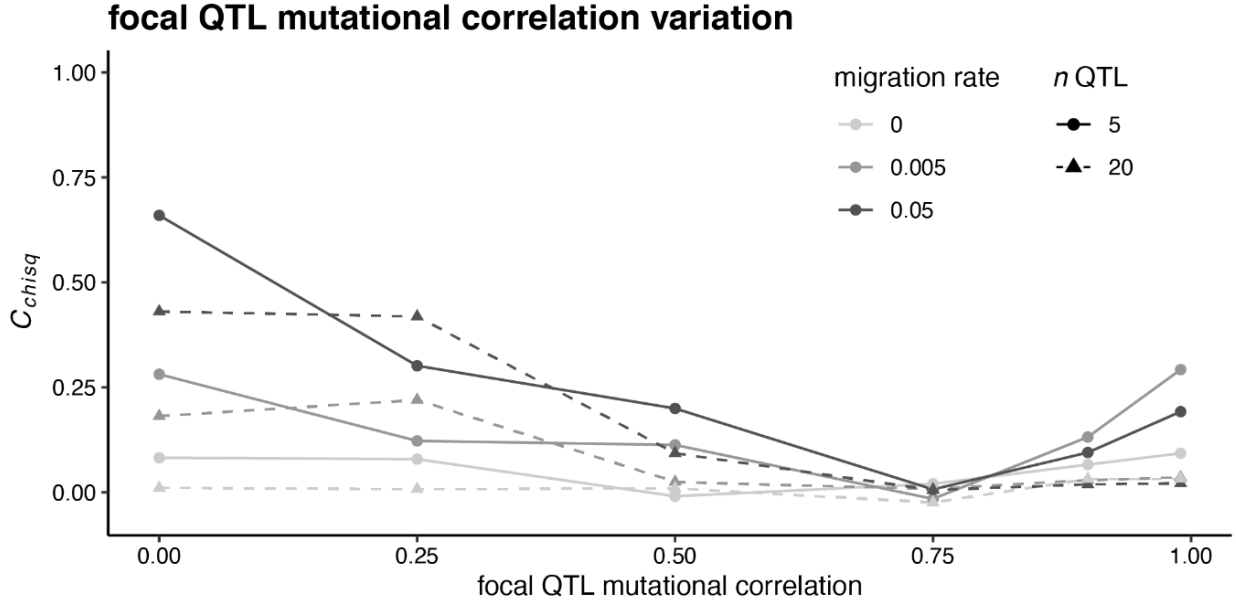

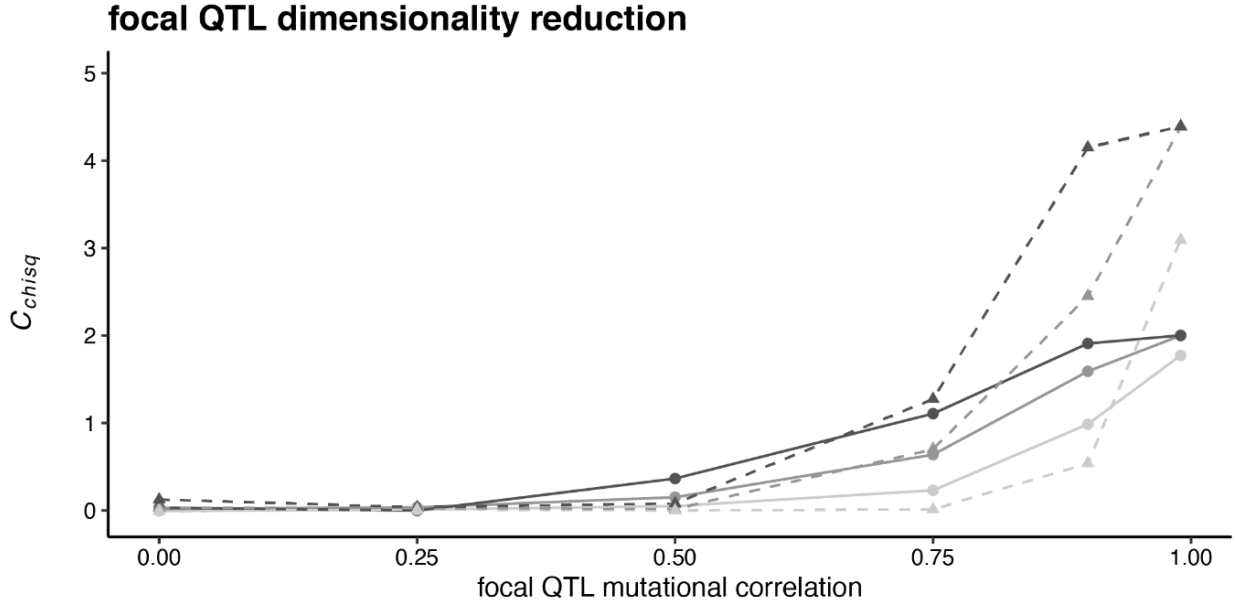

Figure S3. Effects of increasing the number of QTL modelled from five (solid lines, circle points) to 20 (dashed lines, triangle points). In the top pane we examine effect-magnitude variation at the focal QTL (as in fig. 2), with mutational correlations for all QTL fixed at 0.5. In the middle pane we examine mutational correlation variation at the focal QTL (as in fig. 3), with mutational correlations at non-focal QTL of 0.75 and QTL effect magnitudes at 0.5. In the lower pane we examine a reduction in dimensionality at the focal locus (as in fig. 4B), where the total number of phenotypes is two and QTL effect magnitudes are 0.5.